PNAS RESEARCH ARTICLE | PHYSIOLOGY OPEN ACCESS

Sprint-like cardiac dynamics support repeated acrobatic lunges in foraging rorqual whales

Ashley M. Blawas[a,1], James Fahlbusch[a,b], Jack Barkowski[a,b], David E. Cade[a], John Calambokidis[b], Ari S. Friedlaender[c], Brandon Southall[d], Paul J. Ponganis[e], and Jeremy A. Goldbogen[a]

Affiliations are included on p. 8.

Edited by Nancy Knowlton, Smithsonian Institution, DC, Washington; received April 13, 2026; accepted June 22, 2026

The dive response decreases heart rate, regulates blood flow distribution, conserves oxygen, and extends dive duration. In diving animals, dive heart rate can be modulated to meet increased demands of exercise during foraging. However, lunge-feeding rorquals represent an extreme example of exercise under breath-hold conditions: Though most of their dive time is spent gliding and filtering, lunges require high-power, acrobatic sprints to engulf massive volumes of prey-laden water. Our biologging data show that heart rate repeatedly increases with lunging but only gradually declines during filtering, dissimilar from the heart rate-activity coupling observed in other divers. We suggest that the unique nature of rorqual exercise likely requires glycolytic metabolic substrates, rather than aerobic substrates, during short, powerful lunges. During slow filtering, high heart rates may help partially renew these energy sources via oxygen-dependent pathways. By temporarily buffering oxygen demand from supply, the flexible dive response appears to optimize oxygen use in lunging rorquals and support aerobically "cheap" foraging. The data also show that dive cycle heart rate scope increases with rorqual size. We propose that cardiovascular plasticity during high and low power phases of foraging dives underpins rorquals' ability to achieve high foraging efficiencies and combine explosive predation with grazing-like efficiency in a single lineage.

scaling | heart rate | baleen whales | exercise | cardiac function

Significance

Rorqual whales' foraging style combines high- and low-power feeding strategies to exploit prey patches at high efficiencies. To date, limited data exist to assess how rorquals' cardiac function fluctuates to match the "extreme" exercise dynamics of lunge feeding. Our data from blue and humpback whales measured high heart rates with lunging that persist during filtering, supporting continued muscle blood flow despite the limited exercise of gliding. These heart rate patterns mimic those of sprinters, suggesting that high energy lunges rely on anaerobic metabolism and generate an energetic debt only partially paid off during filtering. Increasing cardiac scope with increasing body size further underscores rorquals' cardiac plasticity and highlights the importance of flexible cardiac function for unlocking their unique foraging style.

The ability to match physiological supply to demand sets the limits of animal performance. From the minimum rates of energetic consumption in hibernating bears (1) to the maximum metabolic rates of hovering hummingbirds (2), oxygen (O_2) supply must vary in response to the mass-specific metabolic requirements of tissues, which fluctuate with body size, activity state, and a wide range of environmental factors. For air-breathing vertebrates, the simple act of underwater submersion activates the dive response, lowering and redistributing cardiac output (3). This innate response results in a rapid decrease in heart rate (i.e., bradycardia) and peripheral vasoconstriction, functioning to slow O_2 depletion and preserve endogenous O_2 for hypoxia-intolerant organs like the brain and the heart (4–6). How, and if, divers modulate dive heart rate to meet the metabolic demands of underwater exercise has long been discussed. For diving birds and mammals adapted to maximize effective foraging during breath-hold dives, theoretical models suggest the dive response should fluctuate to support energetically demanding prey search, chase, and capture (7). Empirical data from animals in controlled settings and a few free-ranging scenarios demonstrate that heart rate increases with increasing swimming effort ensuring adequate O_2 delivery to active muscles (8–10). Consequently, a flexible dive response that optimizes the use of lung, muscle, and blood-bound O_2 has replaced the idea of a fixed diving bradycardia, but data as to how this flexibility supports multiple, distinct kinds of underwater exercise in diving birds and mammals remain limited.

Among diving mammals, lunge-feeding rorquals epitomize the physiological challenge of modulating O_2 supply to support extreme exercise during breath-hold diving. Rorquals (Balaenopteridae), including blue whales (*Balaenoptera musculus*) and humpback whales (*Megaptera novaeangliae*), feed by performing repeated high-power lunges at tens to hundreds of meters below the surface, a behavior described as the "largest biomechanical event on Earth" (11). Each feeding lunge requires rapid acceleration of a 10^3 to 10^5 kg animal up to 4 m s^{-1} (12), effective maneuvering, including up to 360° barrel rolls and variable, often steep, pitch angles for optimal body positioning (13), and precisely timed opening and closure of the mouth within seconds of peak approach speed (14). During a lunge, feeding rorquals must meet the concurrent metabolic demands of thrust- and maneuver-generating muscles (15) as well as those of the sensory organs that support visual processing or other means of perceiving prey fields. As turning incurs a higher energetic

Author contributions: A.M.B., P.J.P., and J.A.G. designed research; A.M.B., J.F., J.B., D.E.C., J.C., A.S.F., B.S., and J.A.G. performed research; A.M.B. and J.B. analyzed data; and A.M.B., P.J.P., and J.A.G. wrote the paper.

The authors declare no competing interest.

This article is a PNAS Direct Submission.

Copyright © 2026 the Author(s). Published by PNAS. This open access article is distributed under Creative Commons Attribution-NonCommercial-NoDerivatives License 4.0 (CC BY-NC-ND).

[1]To whom correspondence may be addressed. Email: ashleyblawas@gmail.com.

This article contains supporting information online at https://www.pnas.org/lookup/suppl/doi:10.1073/pnas.2613082123/-/DCSupplemental.

Published July 27, 2026.

Downloaded from https://www.pnas.org by 174.61.233.38 on July 27, 2026 from IP address 174.61.233.38.

cost than straight-line travel (16), energy demand is also expected to increase for lunges with increasing amounts of accumulated maneuvering. Rorquals offset the high power output of lunges with long periods of unpowered filtering, accounting for up to 80% of the lunge cycle in the largest blue whales (17). This results in an intermittent "lunge-and-filter" swimming strategy that is unique among large, air-breathing vertebrate filter feeders. Thus, despite brief periods of very high power output during lunges, rorquals are afforded low metabolic rates during foraging dives (17, 18).

At the cardiovascular level, how rorquals meet the extreme biomechanical demands of lunge feeding during the dive response remains unclear. The only successful study to measure heart rate in a free-ranging diver without prior restraint was in a single blue whale (19). Digital electrocardiogram (ECG) signals and low-resolution dive behavior (only time and depth data sampled at 1 Hz) showed a typical dive response with heart rates during dives as low as 2 beats min^{-1} (bpm) followed by high heart rates, up to 37 bpm, at the sea surface (19). Despite the extreme bradycardia (i.e., a heart rate below resting) observed during dives, heart rate increased 2.5 fold during presumed high-power lunges and gradually decreased during filtering though the absence of high-resolution motion sensors (i.e., accelerometers and magnetometers) and small sample size precluded a complete investigation of this pattern.

Despite the lack of data examining exercise modulation of the dive response in lunge-feeding rorquals, many studies have investigated this question in smaller marine mammals and birds. During some dives, and often during the longest dives, heart rate remains at a "true" bradycardia throughout the bottom phase, despite stroking, prior to the final ascent phase of a dive at which point heart rate increases (20–22). In other dives, especially those shorter than a presumed aerobic dive limit, diving bradycardia is exercise-modulated resulting in positive correlations between activity (e.g., swim speed, stroke rate) and heart rate (8–10). It is important, however, to consider that the high stroke rates and high heart rates of ascent tachycardia can influence such regressions, as can the pulmonary stretch receptor reflex with changes in depth. Though, limited perfusion to muscles helps create the low O_2 conditions necessary for myoglobin to release bound O_2, even species with high myoglobin levels, like emperor penguins and Weddell seals, demonstrate exercise-modulated dive heart rates indicative of muscle blood flow (9, 21). Unlike many smaller divers that graze on small prey and only briefly increase activity for prey search and chase, rorquals employ a unique type of exercise for prey capture that is likely to require distinct exercise-modulation of the dive response. To lunge multiple times within a dive, rorquals perform sprint interval-like accelerations of 15 to 30 s (12) followed by unpowered decelerations of 15 to 90 s (23). Notably, rorqual swimming muscles have predominantly fast twitch muscle fibers with elevated glycolytic (anaerobic) capacity in the superficial layer of the epaxial muscles and predominantly slow twitch fibers with high oxidative (aerobic) capacity in the deep layer, thereby supporting both high and low intensity levels of locomotor activity in the primary swimming muscles (15). Although rorquals have low myoglobin stores (24, 25), their extreme size confers high body O_2 storage and low metabolic rates that should enhance dive time. This distinctive form of exercise and the constraints of large body size thus present a unique test of the flexibility of the dive response.

Here, we aimed to answer the fundamental question of how the combination of extreme body size and high-power feeding impacts the modulation of heart rate during diving. We used multisensor biologgers to measure heart rate and movement in two rorqual species, linking physiological adjustments during a dive cycle to foraging performance and body size in large whales. This study fills a gap in our understanding of how the planet's largest animals integrate biomechanics and cardiovascular control to unlock the metabolic supply that enables their unique filter-feeding foraging style.

Results and Discussion

We leveraged simultaneous measurements of heart rate, kinematics, and body length from blue and humpback whales to evaluate cardiac dynamics during exercise and diving at the upper extreme of animal size and performance. We used data from nine total tag deployments across blue whales in Southern California (n = 4 tags, 946 heart beats) and Monterey Bay (n = 1 tag, 189 heart beats) and humpback whales in both Antarctica (n = 3 tags,15,949 heart beats) and Monterey Bay (n = 1 tag, 464 heart beats) (Table 1 and *SI Appendix*, Fig. S1). ECG measurements captured heart rate across multiple rorqual behaviors and various dive phases (Fig. 1 and *SI Appendix*, Fig. S2). Paired with tag records, unoccupied aerial systems (UAS) allowed for measurements of body length, which were subsequently converted to body mass estimates.

Variability in Heart Rate Dynamics During Rest, Feeding Dives, and Nonfeeding Dives. Several extended humpback tag records allowed for comparison of heart rate across multiple presumed energetic contexts. This included several extended periods of surface logging behavior, when a whale was essentially motionless except during the actual breath, during which a clear respiratory sinus arrhythmia (RSA) was observed (mn250131-66, body length = 12.1 m, body mass = 24,148 kg; Fig. 2). RSA is characterized by a rapid increase in heart rate during inhalation and a gradual decline that stabilizes at a lower heart rate between breaths. In the resting humpback, heart rate peaked at 24.3 ± 2.9 bpm in the first

Table 1. Summary of tag deployments included in this study

Tag ID	Species	Location	Body Length (m)	Body Mass (kg)	Tag Duration (hh:mm:ss)
mn230925-66	Humpback	Monterey	9.4	11,675	11:46:48
mn250131-66	Humpback	Antarctic	12.1	24,148	28:09:46
mn250203-66	Humpback	Antarctic	9.9	13,510	57:47:02
mn250203-67	Humpback	Antarctic	11.4	20,606	18:05:32
bw240625-66	Blue	Channel Is	-	-	1:20:43
bw240629-66	Blue	Channel Is	24.3	92,728	16:39:04
bw240714-66	Blue	Channel Is	20.0	49,198	8:39:35
bw240714-67	Blue	Channel Is	22.2	69,152	8:52:21
bw240909-68	Blue	Monterey	-	-	15:20:16
TOTAL					178:37:23

For each deployment, the tag ID, species, study location, measured body length, estimated body mass, and total tag duration are reported

Downloaded from https://www.pnas.org by 174.61.233.38 on July 27, 2026 from IP address 174.61.233.38.

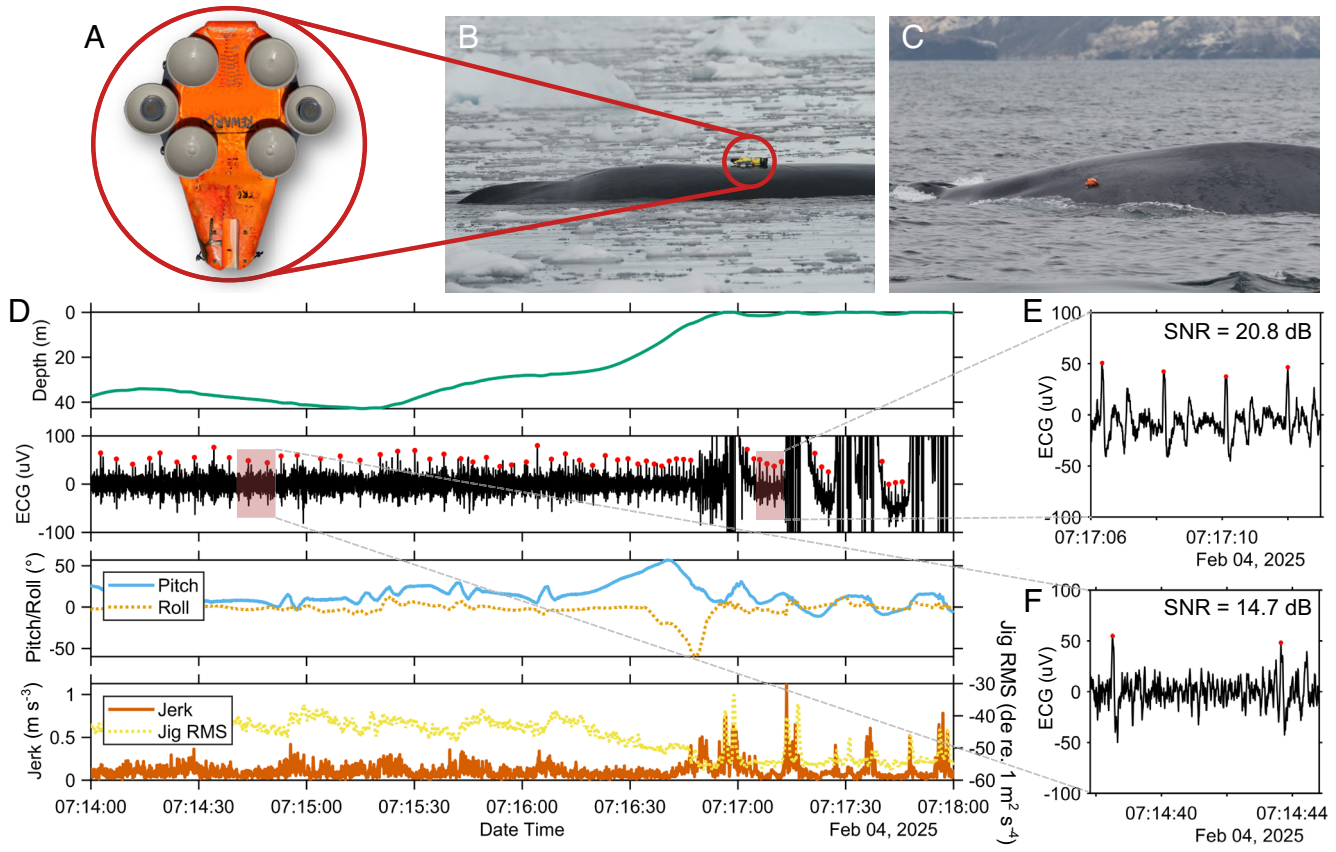

Fig. 1. A custom suction cup-attached ECG tag (*A*) deployed on a humpback whale (*B*) and blue whale (*C*). Depth, the electrocardiogram (ECG), pitch and roll, and jerk signals presented for 4 min during the second half of a dive to 40 m and the early postdive interval from a humpback whale (mn250203-67). Jerk is calculated as the rate of change of three-axis acceleration and Jig RMS is derived from high-frequency acceleration as previously described (26). (*D*) Artifacts are present in the ECG signal during surfacings and heart rate remains elevated during brief submersions between breaths. Zoomed in ECG data is shown during a surfacing (*E*) and at depth (*F*). Signal to noise ratio (SNR) is presented for both ECG data segments as calculated by 20 $\log_{10}$(S N^{-1}) where S is the amplitude of the signal and N is the standard deviation of the baseline noise.

30 s after each breath and declined to 15.4 ± 3.4 bpm between breaths, oscillating between 11.1 and 19.3 bpm. A pronounced RSA further reinforces robust parasympathetic regulation at rest, consistent with strong vagal tone reported in other divers. A gray whale calf undergoing rehabilitation demonstrated similar patterns at rest with respiration-driven oscillation between 30 to 40 bpm (during breathing) and 15 to 20 bpm (between breaths) (27). In adult and pup northern elephant seals, RSA occurred during normal breathing periods linked to sleep apnea, but after long apneas heart rate initially remained high, with the arrhythmia becoming more pronounced as normal breathing continued (28, 29). In bottlenose dolphins, elevated heart rate after long breath holds was only replaced by a clear RSA when exhaled CO_2 declined to normal levels (30), suggesting some utility in this pattern for assessing recovery from diving and foraging.

Although the exact physiological mechanisms that underpin the heart rates observed during the RSA remain incompletely understood, they likely represent the closest approximation of resting heart rate in an intermittent breather (32). Mean heart rate of the humpback during this logging period, the first estimate of resting heart rate in a free-ranging, fully aquatic marine mammal, was 18.5 ± 5.4 bpm, which agrees with the allometric prediction of 19.3 bpm (31) for a resting terrestrial mammal of comparable size (Fig. 2). The breathing rate of 38.8 ± 15.1 breaths h^{-1} during logging was low compared to predictions for basal respiratory rate in fully aquatic mammals (50.2 breaths h^{-1} at −1 °C) (33) but within expected variability (±1 SD). This breathing rate closely matched mean values reported from humpbacks on breeding grounds (42 ± 12 breaths h^{-1}) (34) and was notably lower than that from feeding grounds (61.2 ± 3.3 breaths h^{-1}) (18). This suggests that energetic demand on the breeding grounds may be close to resting metabolic rate and reinforces that low physiological states can be achieved during resting between foraging bouts which occupy, on average, 6% (range: 0 to 41%) of time spent on feeding grounds (34). Ultimately, the resting heart rate and breathing rate measured here reinforce the view that baleen whales exhibit comparable metabolic rate scaling to that of terrestrial mammals (17) and provide a useful baseline for accurately assessing bradycardia (heart rates <18.5 bpm) and tachycardia (heart rates >18.5 bpm) in this individual (or similarly sized humpbacks).

In another humpback (mn250203-66, body length = 9.9 m, body mass = 13,510 kg), our recording included multiple hours of both nonfeeding and feeding behavior, allowing us to make comparisons of heart rate across activity levels. During 2 h of nonfeeding dives of the humpback whale, surface heart rates had a mean value of 29.3 ± 3.6 bpm (range: 25.0 to 32.4 bpm) (Fig. 3*A*). Heart rate patterns at depth displayed the typical dive response with low heart rates of 13.1 ± 2.4 bpm (range: 9.8 to 15.8 bpm) during the bottom phase of dives. Although brief data gaps in heart rate occurred during descents, the limited duration of these gaps suggests similar trends in descent and ascent heart rate patterns to other divers (20, 21) and the previous blue whale heart rate recording (19). Specifically, heart rate decreased (at approximately 0.8 to 1.2 bpm s^{-1}) to a low value upon submersion (1st quantile of 6.7 bpm during descent

Downloaded from https://www.pnas.org by 174.61.233.38 on July 27, 2026 from IP address 174.61.233.38.

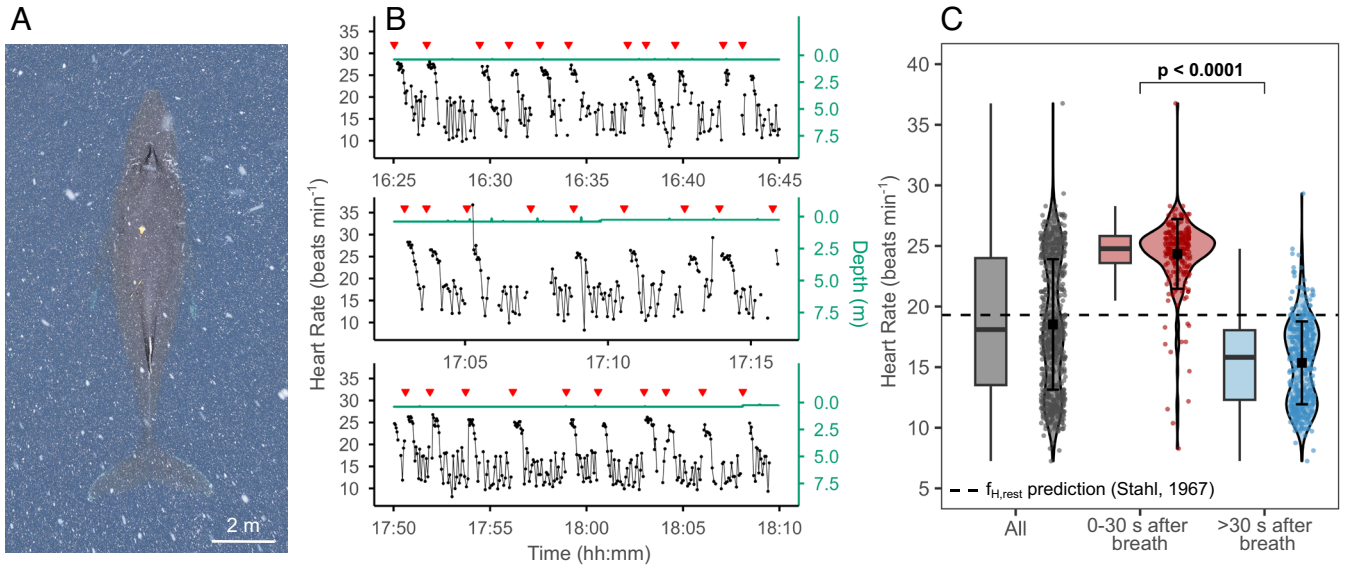

Fig. 2. Resting heart rate of a humpback whale. Heart rate of a humpback whale (mn250131-66, body length = 12.1 m, body mass = 24,148 kg: (*A*) at rest demonstrates respiratory sinus arrhythmia (RSA) during three extended surface intervals (*B*). Red arrows indicate the timing of breaths and depth is represented by a green line. Heart rate is plotted by black points and lines. All instantaneous heart rates (black) and instantaneous heart rates in the first 30 s (red) compared to those >30 s after a breath (blue) (*C*). Boxplots show the quartiles of each distribution with the thick line indicating the median value and the shaded region representing the 25th to 75th quartiles. Violin plots with jittered points show the full data range with black squares indicating the mean value and error bars indicating the standard deviation. The black dashed line indicates the allometric prediction of resting heart rate for this individual of 19.3 beats min^{-1} (31). The result of a Wilcoxon rank sum test to compare the instantaneous heart rate distributions of the RSA is included.

phase), remained low at depth, and increased gradually (at approximately 0.6 to 0.8 bpm s^{-1}) during ascent (mean ascent heart rate of 20.8 ± 5.0 bpm) with a distinct anticipatory tachycardia in the final ascent stage (99th quantile of 31.1 bpm during ascent phase). Observed rates of heart rate decline were on the slow end of those measured in other, smaller marine mammals (35). Following several deeper nonfeeding dives, the humpback's surface heart rate remained distinctly elevated, suggesting prolonged recovery after an extended submergence. At depth, instantaneous heart rate also showed a clear relationship with instantaneous depth, and deeper dives were accompanied by correspondingly lower heart rates, reinforcing depth-dependent modulation of the dive response. It is likely that dive duration, or perhaps anticipated dive duration, also plays a role in modulating dive heart rate though this dataset did not include conditions under which the effects of dive depth and duration could be disentangled.

Overall mean instantaneous heart rate during shallow-feeding and deep-feeding of the humpback whale represented a 73.2%

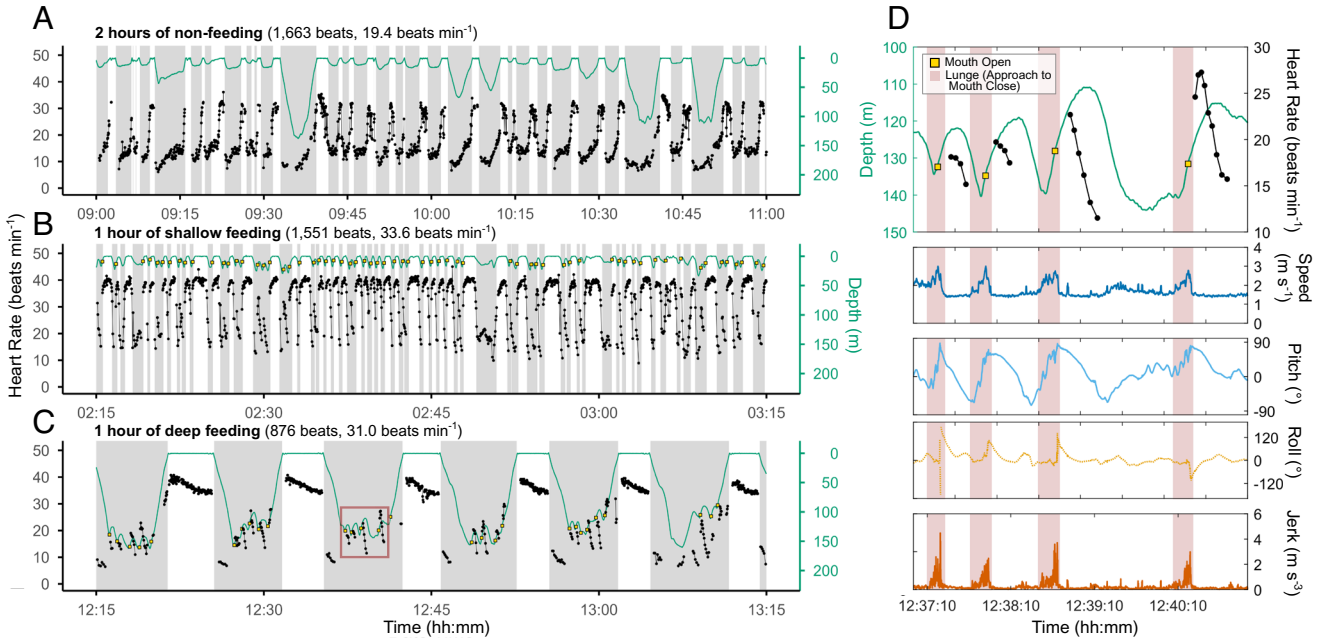

Fig. 3. Humpback whale heart rate across behavioral states. Heart rate of a humpback whale (mn250203-66) during nonfeeding (*A*), shallow feeding (*B*), and deep feeding (*C*). Depth is represented by a green line and lunges (mouth open) are marked with yellow squares. Heart rate is plotted with black points and lines. Gray boxes indicate where depth was >2 m. A zoomed in portion of heart rate and depth during deep feeding lunges (*D*) with kinematics corresponds to the red box in (*C*). Kinematics shown are speed, derived from high-frequency accelerometer "jiggle" (36), pitch, roll, and jerk (calculated as the rate of change of three-axis acceleration). Highlighted pink areas indicate lunges, from the approach to mouth close, and yellow squares indicate mouth opening.

Downloaded from https://www.pnas.org by 174.61.233.38 on July 27, 2026 from IP address 174.61.233.38.

(33.6 vs. 19.4 bpm) and 59.8% (31.0 vs. 19.4 bpm) increase from mean instantaneous heart rate during nonfeeding. Generally, surface heart rates were higher between feeding dives than between nonfeeding dives. During an hour of shallow feeding, surface heart rates remained high, at 39.3 ± 1.7 bpm (range: 37.8 to 40.7 bpm) within brief surface intervals that rarely contained more than one breath (Fig. 3*B*). In contrast, surface heart rate between deep feeding dives, which had a mean value of 36.3 ± 1.8 bpm, demonstrated a distinct trend of recovery from an initial maximum of 39.9 bpm to 32.9 bpm (99th and 1st quantiles) during 3 to 4 min surface intervals containing 6 to 10 breaths (Fig. 3 *C* and *D*). During shallow feeding, there were few instances when it was possible to measure heart rate at depth, but generally heart rate on descent leading up to the lunge reached a low value of 10.9 bpm (1st quantile) before the signal was lost due to noise during rapid fluking (Fig. 3*B*). In contrast, heart rate during the bottom phase of deep feeding dives demonstrated higher variability (range: 11.6 to 22.9 bpm) during subsequent filtering phases of repeated lunges (Fig. 3 *C* and *E*), but reached its lowest values of approximately 6.6 bpm (1st quantile) at the end of descents (Fig. 3 *C* and *F*). Heart rate during feeding therefore appears to be modulated by depth (i.e., lower heart rates at deeper depths), similar to that of nonfeeding dives, yet the effect of lunge feeding results in an increase in heart rate. Like heart rates during nonfeeding periods, dive duration may also exert an effect on this trend whereby heart rate is lowered in anticipation of a given dive duration but as deeper feeding dives were also longer in our dataset, we were unable to explore this hypothesis further.

Rorqual Lunging Heart Rates. Heart rate immediately following a lunge was elevated to 21.9 bpm (95% CI: 19.6 to 24.2 bpm from 65 postlunge HR traces) in blue whales and 28.2 bpm (95% CI: 27.4 to 28.9 bpm from 124 postlunge HR traces) in humpback whales as predicted by the best fit generalized additive model (Fig. 4 *A* and *B*). Following a lunge, heart rate tended to gradually decline throughout the filter phase, which takes, on average, 60 s for blue whales and 17 s for humpback whales (23). The predicted heart rate of a blue whale 60 s after the lunge was 7.7 bpm, while that of a humpback was 19.0 bpm 17 s after a lunge. For long filtrations of 101 s and 29 s (mean + 2 * SD) (23), predicted heart rates were even lower at 5.6 bpm and 14.6 bpm for a blue and humpback whale. Thus, heart rate at mouth open (i.e., the end of the acceleration phase and initiation of engulfment) was 2.8 and 1.5 times the rate measured at the end of the filter phase, in blues and humpbacks, respectively, or, for the longest filter phases, 3.9 and 1.9 times the low heart rates postfiltering. For the blue whales in this study, this increase of 2.8 times postfilter heart rate is similar to that previously observed in lunging blue whales of 2.5, while the increase for humpbacks in this study of 1.5 times postfilter heart rate was lower (19). Notably, while humpbacks postlunge heart rate of 28.2 bpm was clearly tachycardic compared to a resting heart rate of 18.5 bpm, this only represents a 1.5 times increase in heart rate compared to the >2 times increase in heart rate observed in sprinters compared to a pre-exercise period (37). In contrast, the postlunge heart rate of humpbacks was 2.2 times the mean bottom phase heart rate (13.1 bpm) during nonfeeding observed in an extended record. While it is difficult to assess what the most accurate comparison of heart rate dynamics between sprinters and lunging rorquals may be, equivalent increases in heart rate in an individual selectively perfusing a subset of tissues compared to one perfusing all tissues are unlikely to represent equivalent increases in tissue O_2 delivery. Between repeated sprints or lunges, however, sprinters maintain higher relative heart rates compared to rorquals and therefore may provide more continuous perfusion to

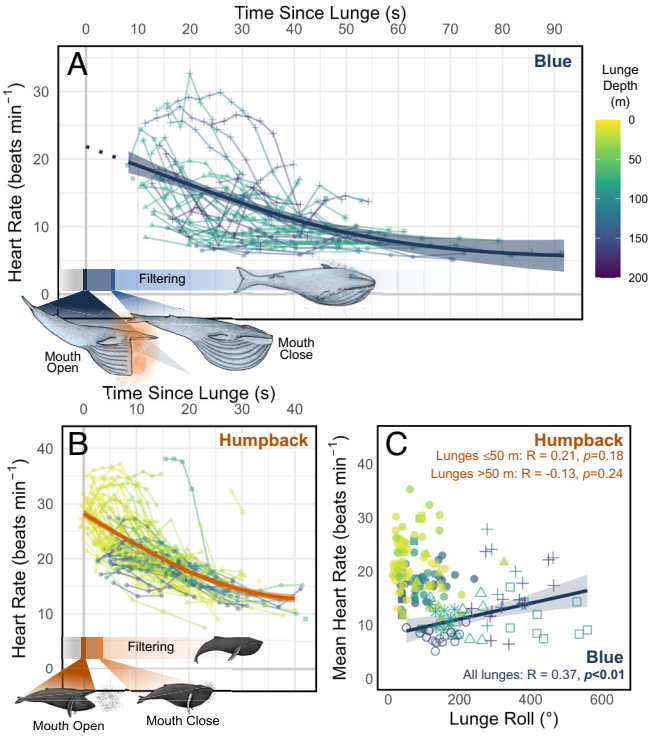

Fig. 4. Postlunge heart rates of rorquals. Heart rate traces following lunges for blue (dark blue) (*A*) and humpback (orange) whales (*B*). Solid lines represent the generalized additive model that best fits the data determined via the iteratively reweighted least squares algorithm with k = 5 across the data range. The dashed line indicates the projection of the GAM to y = 0 if the data range does not include 0. (*C*) Accumulated roll during the lunge approach versus mean heart rate of each trace following lunges with blues plotted as open/line markers and humpbacks as closed markers. The correlation coefficient (R) and *P*-value for the slope (*p*) are shown for linear regressions of lunge roll and mean heart rate. Linear regressions with a slope significantly different from 0 and their 95% CIs are plotted. The color of each trace or point indicates the depth of the lunge. Each individual within a species is indicated by a different shape.

the skeletal muscles (37). Future efforts to constrain estimates of fractional cardiac output to the skeletal muscles based on changes in heart rate will be valuable to better align comparisons between exercise with and without submersion.

In both species, postlunge heart rate patterns could be characterized into two stereotypical patterns. The first pattern was marked by a, generally, high local maximum in heart rate that distinctly plateaued before decreasing. The second pattern consisted of a gradual, monotonic decrease, with lower heart rates directly following the lunge than the former pattern. In humpback whales, the former was more frequently associated with shallow lunges (<50 m), whereas the latter predominated following deeper lunges (Fig. 4*B*). Although occasional gaps in heart rate, particularly during lunge approaches, do not exclude the possibility that transient high heart rates immediately after deep lunges of humpbacks may be missed, the divergence of observed heart rate trajectories by depth is evident. Depth, possibly via lung compression and stretch receptor reflexes, may contribute to high heart rates at shallower depths in the humpback whales. These high heart rates would allow for greater lung O_2 extraction, thus potentially increasing the overall accessible O_2 stores during shallow dives. Notably, while the sample size of lunges and the variation in lunge depth for blue whales was limited, the appearance of these two patterns varied more by individual than by lunge depth, with only one blue whale (bw240909-68) displaying distinct plateauing of high heart rates (Fig. 4*A*).

Downloaded from https://www.pnas.org by 174.61.233.38 on July 27, 2026 from IP address 174.61.233.38.

Investigations of heart rate in smaller marine mammals demonstrate the flexibility of the dive response. During short, aerobic dives heart rate increases with increasing activity to optimize the use of both blood- and muscle-bound O_2 and maximize aerobic dive limit (8), while in longer dives activity and heart rate become decoupled to conserve blood O_2 for the brain and, secondarily, the muscles increasingly rely on myoglobin and eventually glycolysis. The heart rate patterns of lunging rorquals in this study further reinforce the flexibility of the dive response. The nature of lunging rorqual "sprints" requires rapid, powerful contractions of fluking muscles for 15 to 30 s (12) which may outstrip the capacity for mitochondrial production of ATP in the predominantly glycolytic (15) and low myoglobin-containing (24, 25) locomotor muscles of rorquals. In these conditions, the muscle could rely on phosphocreatine breakdown and glycolysis to generate energy. While the glycolytic system requires minutes of recovery, phosphocreatine can be rapidly resynthesized to 65 to 90% of resting levels in 60 to 120 s (38–40). We propose that high postlunge heart rates persisting into the filtering phase support continued muscle blood flow that may help replenish muscle O_2 and, at least partially, phosphocreatine between repeated lunges. High heart rates despite low levels of instantaneous activity during filtering may be necessary to restore energy substrates that become depleted and cannot be actively replenished within the short duration of the lunge itself. Even higher postlunge heart rates could be needed following subsequent lunges within a single dive to provide sufficient O_2 if the replenishment of O_2 and phosphocreatine is only partial (*SI Appendix*, Fig. S3). Recent work in belugas and dolphins in professional care provides evidence that metabolic products accumulate with increasing exercise repetitions (41) reinforcing this possibility in large whales.

In blue whales, accumulated roll during the lunge, a key kinematic measure that distinguishes different types of lunge feeding events (13) was positively correlated ($R = 0.37$, $P < 0.01$) with mean postlunge heart rate. This suggests that the mechanical work of maneuvering can increase heart rate, at least for the lunges captured in these records which all occurred at depths >50 m (Fig. 4*C*). There was no relationship between accumulated lunge roll and mean postlunge heart rate in humpbacks, which may be a result of more limited rolling, typically less than 180°. Nevertheless, the correlation coefficient between accumulated lunge roll and mean postlunge heart rate was notably higher for deep ($R = 0.21$, $P = 0.18$) compared to shallow lunges ($R = -0.13$, $P = 0.24$) in humpbacks. Rorquals are known to maneuver more when foraging on low-density prey, presumably to maximize intake from the prey patch (42). If increased maneuvering does come at a higher energetic cost, then acrobatic lunges may be used selectively to increase foraging efficiency or when O_2 is readily accessible (i.e., near the surface). The lack of an association between postlunge heart rate and accumulated roll, particularly for shallow lunges, in humpbacks could reflect sustained perfusion of the lungs and continued O_2 supply, further highlighting the dive response's optimization of O_2 use for the "nature of a given dive" (43).

The Effect of Body Size. Heart rate plays a critical role in modulating O_2 supply to the tissues. We have shown that in lunge-feeding rorquals, like other divers and terrestrial mammals, high hearts are important for matching the increased power demands of exercise during foraging. Yet, rorquals face unique constraints of their extreme body size; in particular, low mass-specific field metabolic rates (17) that are roughly 2 times their allometrically predicted basal metabolic rate (BMR) (44). This compares to field metabolic rates that are roughly 6.0 times BMR for foraging otariids and dolphins (45), 5.2 times BMR in hummingbirds (46), and 4.1 to 5.6 times BMR in Tour de France cyclists (47). Instead, rorquals seem to be foraging at similar metabolic rates to juvenile northern elephant seals and Weddell seals at sea which are, on average, 1.3 (range: 0.9 to 2.4) times and 1.5 times predicted BMR (48, 49). Because of this energetic ceiling, mass-specific O_2 consumption in foraging rorquals must remain, on average, low despite the very brief but very high-power (50 times BMR) required for lunging (50). Our data show that the unique style of exercise demanded by underwater lunge-feeding may remain aerobically "cheap," in part, by largely relying on glycolysis/phosphocreatine metabolism in highly glycolytic locomotor muscles, thus spatially and temporally buffering the muscle's need for O_2. High postlunge heart rates provide a mechanism to rapidly restore, at least partially, local O_2 stores and energy substrates while high postdive surface heart rates facilitate more complete O_2 renewal and purging of CO_2. The ability to achieve finely tuned O_2 delivery rates ideally matched to these transient increases in demand would thus benefit rorquals to maximize the efficiency of O_2 transport and, in turn, aid in minimizing aerobic demand.

Divergent allometric scaling of typical minimum ($b = -0.29$) and maximum ($b = -0.20$) heart rates in blue and humpback whales (Fig. 5*A*) results in a heart rate scope during routine diving activity that increases with body size ($b = 0.09$, Fig. 5*B*). Empirical measurements from pinnipeds and small cetaceans match these trends (51, 52). At large body sizes, rorquals are afforded large typical heart rate scopes among diving mammals with blue whales achieving larger diving heart rate scopes than humpbacks during routine diving. Thus, rorqual heart rate allometry suggests an additional mechanism by which these large-bodied divers may minimize aerobic demand. By achieving highly incremental control of cardiac output (i.e., a larger dynamic range) at large body sizes, heart rate can vary more on short timescales to support fluctuations in energy demand.

Because limited information exists on the kinematics and energetics of foraging in large-bodied odontocetes as well as O_2 storage in large whales more broadly, it is difficult to hypothesize about what these findings may mean for rorquals' toothed counterparts. We suspect that cardiac scope in other free-ranging cetaceans will depend on the magnitude and distribution of O_2 stores, muscle fiber type distribution, fiber recruitment during a particular activity, and the effort of that activity. It is possible, if odontocetes store higher proportion of body O_2 in muscle and/or have generally enhanced O_2 stores, modulation of heart rate with exercise at depth might be comparatively limited if low perfusion creates the local conditions required for myoglobin to release O_2. In this case, cardiac scope in large, deep-diving toothed whales may be less relevant than in rorquals, but more data on O_2 supply and demand in these species is needed for cross-taxa comparisons.

We show that large heart rate scope is not only a byproduct of large size in rorquals, but perhaps a prerequisite for balancing the extreme biomechanical demand of rorqual feeding while maintaining low field metabolic rates. By matching some of the highest absolute and lowest mass-specific metabolic demands observed across marine mammals with commensurate O_2 supply, rorquals balance a fundamental energetic trade-off and combine explosive predation with grazing-like efficiency in a single lineage.

Materials and Methods

Tag Data Collection. Animal-borne suction cup attached tags equipped with ECG recorders were deployed on nine individuals (five blue whales and four humpback whales) between 2023 and 2025. Two configurations of custom-built tags were used: Configuration A included a custom-built ECG recorder/ housing

Downloaded from https://www.pnas.org by 174.61.233.38 on July 27, 2026 from IP address 174.61.233.38.

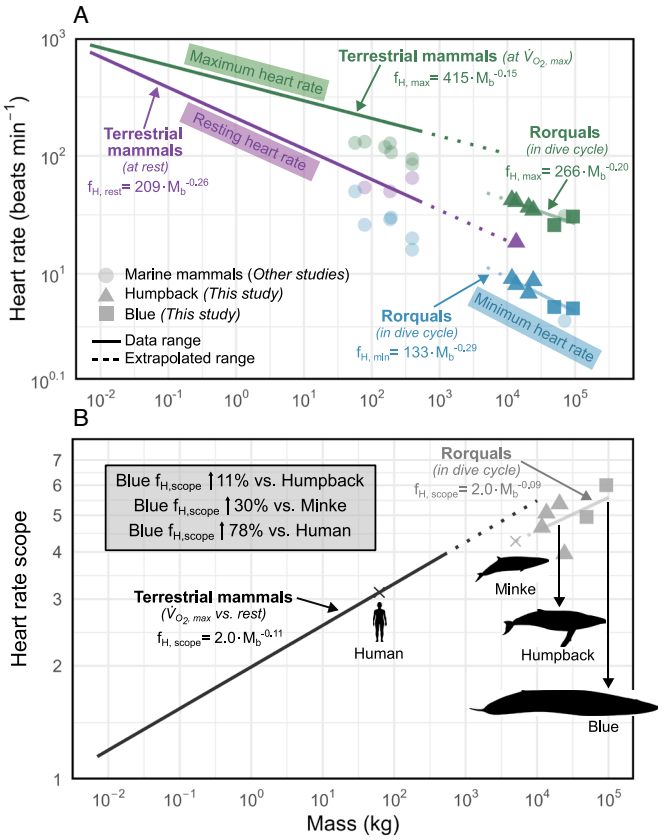

Fig. 5. Heart rate allometry in rorquals. (*A*) Allometric scaling relationships between body mass and heart rate for rorquals and terrestrial mammals. For rorquals, data points for maximum heart rate (green), resting (purple), and minimum heart rate (blue) measured during the dive-surface cycle in this study are shown for blue whales (squares) and humpback whales (triangles). Data points from other studies of marine mammals are included as semitransparent circles. Linear fits derived via ordinary least squares regression are presented to describe the relationship between heart rate and body mass in rorquals in addition to published scaling relationships from terrestrial mammals for maximum heart rate at $\dot{V}_{O2,\,max}$ (green) and resting heart rate (purple). Solid lines indicate the data range of each regression, and dashed lines represent its extrapolation to the range of typical group body sizes. (*B*) Heart rate scope allometric scaling for rorquals (maximum/minimum heart rate in the dive cycle; gray) and terrestrial mammals (maximum at $\dot{V}_{O2,\,max}$/minimum at rest heart rate; black). As the conditions under which maximum, resting, and minimum heart rates were measured in terrestrial mammals and rorquals differ, these lines are not intended to be compared directly but rather provide a conceptual exercise illustrating the underlying trends. Blue whales (squares) and humpback whales (triangles) are shown along with X's indicating predicted values from the respective regression lines for human heart rate scope at a mass of 62 kg (53) and minke whale heart rate scope (at a mass of 5,534 kg at 7.7 m) (54, 55). Terrestrial mammal heart rate scaling data are from Weibel et al., (56). Data from other marine mammals include harbor porpoises (57), California sea lion (58), bottlenose dolphins (59), Northern elephant seals (28), Weddell seals (60), Southern elephant seals (61), gray seals (20), and a blue whale (19).

(UFI/Meer Instruments) incorporated into a suction cup attached tag (CATS Diary WiFi; Customized Animal Tracking Solutions) and Configuration B included an off-the-shelf kinematics/ECG recorder/housing (Little Leonardo) incorporated into a suction cup attached float (CATS Float; Customized Animal Tracking Solutions). Data were recorded at 100 Hz and 250 Hz for ECG, 400 Hz and 100 Hz for 3-axis acceleration, and 10 Hz and 1 Hz for pressure and temperature in Configuration A and Configuration B, respectively. Configuration A also recorded 50 Hz data from a 3-axis gyroscope and a 3-axis magnetometer. The ECG recorders were connected to two Ag/AgCl surface electrodes (12 mm diameter × 1 mm Ag/AgCl Sintered Silver Disk Electrodes; Biomed Electrodes, Fair Oaks, CA) housed in custom spring-damped extensions on either side of the tag float and enclosed by small silicone suction cups for attachment and larger silicone suction cups for additional flow dampening.

The tags were attached using a 6-m carbon fiber pole and a 6.3-m inflatable boat in Monterey Bay, California, the Channel Islands, California, and the Western Antarctic Peninsula following the tagging procedures described previously (62). The tags were intentionally deployed on the animal's left side, as low as possible to attempt to access a cardiac window where ECG amplitudes were assumed to be larger; however, tags were ultimately placed opportunistically upon approach (*SI Appendix*, Fig. S1).

Within the timeframe in which these nine successful tag deployments occurred, tags were deployed on rorquals in 20 separate instances with 11 records containing no high-quality ECG signal. The ability to successfully record heart rate in a large, free-swimming baleen whale without prior restraint for ECG electrode placement is nontrivial and remains a technical and logistical challenge for which further engineering development is needed. A better understanding of the effect of the tag's location on the body on ECG signal amplitude and the elimination of noise generated by high-frequency movement ("jiggle") of the tag at high speeds remain two critical avenues for ECG biologger improvement. Still, a 45% success rate (i.e., 9/20 records containing high-quality ECG) represents a major advance in the reliability of existing ECG biologgers for baleen whales.

Body Size Measurements. In 2023 and 2024, we used a DJI Phantom 4 Advanced to collect 126 images of four blue whales and one humpback whale. 22 images were of sufficient quality for measurements of body length. In 2025, we used two DJI Mavic 3 Pros and one Freefly Astro to collect 39 images of four humpback whales, 23 of which we used for measurements of body length. We evaluated image quality using the criteria described in Christensen et al., (63). Camera specifications like focal length and sensor width were provided by the manufacturer. Altitude measurements were collected using a laser altimeter. If laser altimeter data were not available, the on-board barometer of the drone was calibrated using measurements of a calibration object. Calibration object measurements and altitude corrections were done on a flight-by-flight basis (64). Good quality photogrammetry images were used to calculate total length (TL) in meters, from rostrum to fluke notch, using MorphoMetriX (65). Each tagged whale had multiple good quality images from which to derive measurements so we used an average total length across all images to report body lengths. From real-world unit measurements of individual length, we then used previously published regressions of body length to body mass for blue whales (54) and humpback whales (66) to estimate the body mass of all individuals in the study.

Tag Data Analysis. Pressure and kinematic data were analyzed using established methods that rely on custom MATLAB scripts to convert raw measurements into usable data streams (26). In brief, pressure was adjusted based on the internal temperature of the tag and then calibrated using in situ surface measurements. The acceleration and magnetic field measurements were calibrated using an in situ spherical calibration method, converted from the tag frame of reference into the whale frame of reference, and corrected for instances where the tag orientation changed on the animal (i.e., a tag slip). Forward speed was derived using the established accelerometer jiggle approach by calibrating high-frequency variation in acceleration against vertical depth rate (36).

Individual lunge feeding events were analyzed for approach, engulfment, and filtering phases (14). The start of the approach was defined as the start of continuous fluking directly preceding the lunge, mouth open as the peak in speed, mouth close as the point after the sharpest deceleration in speed and as the beginning of the filtration phase, and end of filtering as the start of fluking or increase in jerk associated with rapid increases in body movement, whichever occurred first (23). The goal of this definition for filtering was to ensure filtering represents only unpowered, low movement behavior. Accumulated lunge roll was calculated as the summed absolute value of the difference in instantaneous roll from the start of the approach to the end of filtering.

Analysis of ECG data followed established protocols described previously (19). All ECG records were audited manually to identify R-peaks by locating distinct and repeatable ECG waveforms. Instantaneous heart rate was determined by comparing the time interval between two successive beats. Where noise prohibited the detection of beats from the ECG data, a gap was noted, and the calculation of instantaneous heart rate resumed at the next instance that two successive beats with no gap were observed. Maximum and minimum heart rates were calculated as the 1st and 99th quantiles of all recorded instantaneous heart rate

Downloaded from https://www.pnas.org by 174.61.233.38 on July 27, 2026 from IP address 174.61.233.38.

measurements for each deployment. All ranges are reported as the 10th to 90th quantiles to ensure robustness of outliers unless otherwise stated. Postlunge heart rates were defined as the first instantaneous heart rate measurement occurring no earlier than 2 s before mouth opening, allowing inclusion of early beats that were sometimes, though rarely, visible at the end of the approach phase.

Breaths were assessed as the co-occurance of depth minima, local peaks in jerk, and local peaks in animal pitch angle as has been used previously (67, 68).

Statistical Analysis. All statistics were conducted in R (v 4.5.1) (69). We modeled changes in heart rate following lunging using generalized additive models (GAMs) fit by the *mgcv* package (70) with time since lunge as our smoothed predictor. Models were determined via the iteratively reweighted least squares algorithm with k, the basis dimension parameter, equal to 5. The model assumed normally distributed residuals (Gaussian family). Ordinary least squares regression (*stats* package) was used to assess the relationship between lunge roll and mean lunge heart rate and a Wilcoxon rank sum test was used to compare heart rates in the first 30 s after a breath to those >30 s after a breath during the logging period with a distinct respiratory sinus arrhythmia. An $\alpha = 0.05$ was used to assess significance for all statistical tests.

Data, Materials, and Software Availability. Data used in the study are available at https://doi.org/10.25740/gc221hc9325 (71).

ACKNOWLEDGMENTS. We thank the entire crew and science team aboard the R/V Shearwater (Santa Barabara) and the M/Y Argus during data collection. We are grateful to the Duke Marine Robotics and Remote Sensing Lab for their contributions and expertise. All work was conducted under approval of the National Marine Fisheries Service (Permit 27911) and the Antarctic Conservation Act (2025-019 Permit) and Institutional Animal Care and Use Committee protocols. The work was supported by an Office of Naval Research Grant (N000142312561). Data collection in Southern California was supported by The Sound & Marine Life Joint Industry Program, Bureau of Ocean Energy Management, and the Office of Naval Research. Data collection in the Antarctic was supported by the MAC3 Impact Philanthropies, Pelorus, and the Blundy Family.

Author affiliations: [a]Hopkins Marine Station, Oceans Department, Stanford University, Pacific Grove, CA 93950; [b]Cascadia Research Collective, Olympia, WA 98501; [c]Oceans Sciences Department, University of California, Santa Cruz, CA 95064; [d]Southall Environmental Associates, Inc., Aptos, CA 95003; and [e]Center for Marine Biotechnology and Biomedicine, Scripps Institution of Oceanography, University of California San Diego, La Jolla, CA 92037

1. Ø. Tøien *et al.*, Hibernation in black bears: Independence of metabolic suppression from body temperature. *Science* **331**, 906–909 (2011).
2. P. Chai, R. Dudley, Limits to vertebrate locomotor energetics suggested by hummingbirds hovering in heliox. *Nature* **377**, 722–725 (1995).
3. W. M. Zapol *et al.*, Regional blood flow during simulated diving in the conscious Weddell seal. *J. Appl. Physiol.* **47**, 968–973 (1979).
4. L. Irving, Respiration in diving mammals. *Physiol. Rev.* **19**, 112–134 (1939).
5. P. F. Scholander, Experimental investigations on the respiratory function in diving mammals and birds. *Hvalradets Skrifter* **22**, 1 (1940).
6. P. F. Scholander, The master switch of life. *Sci. Am.* **209**, 92–107 (1963).
7. R. W. Davis *et al.*, The diving paradox: new insights into the role of the dive response in air-breathing vertebrates. *Comp. Biochem. Physiol. A Mol. Integr. Physiol.* **138**, 263–268 (2004).
8. R. W. Davis, T. M. Williams, The marine mammal dive response is exercise modulated to maximize aerobic dive duration. *J. Comp. Physiol. A* **198**, 583–591 (2012).
9. T. M. Williams *et al.*, Exercise at depth alters bradycardia and incidence of cardiac anomalies in deep-diving marine mammals. *Nat. Commun.* **6**, 6055 (2015).
10. B. I. McDonald, M. S. Tift, L. A. Hückstädt, M. Jeffko, P. J. Ponganis, Stroke effort and relative lung volume influence heart rate in diving sea lions. *J. Exp. Biol.* **223**, jeb214163 (2020).
11. P. F. Brodie, Noise generated by the jaw actions of feeding fin whales. *Can. J. Zool.* **71**, 2546–2550 (1993).
12. J. A. Goldbogen *et al.*, Scaling of lunge-feeding performance in rorqual whales: Mass-specific energy expenditure increases with body size and progressively limits diving capacity. *Funct. Ecol.* **26**, 216–226 (2012).
13. J. A. Goldbogen *et al.*, Underwater acrobatics by the world's largest predator: 360° rolling manoeuvres by lunge-feeding blue whales. *Biol. Lett.* **9**, 20120986 (2013).
14. D. E. Cade, A. S. Friedlaender, J. Calambokidis, J. A. Goldbogen, Kinematic diversity in rorqual whale feeding mechanisms. *Curr. Biol.* **26**, 2617–2624 (2016).
15. J.-L.L. Rivero, Locomotor muscle fibre heterogeneity and metabolism in the fastest large-bodied rorqual: The fin whale (Balaenoptera physalus). *J. Exp. Biol.* **221**, jeb177758 (2018).
16. R. P. Wilson *et al.*, Turn costs change the value of animal search paths. *Ecol. Lett.* **16**, 1145–1150 (2013).
17. A. M. Blawas *et al.*, Life in the slowest lane: Feeding allometry lowers metabolic rate scaling in the largest whales. *Sci. Adv.* **11**, eadw2232 (2025).
18. S. K. A. Videsen *et al.*, Cheap gulp foraging of a giga-predator enables efficient exploitation of sparse prey. *Sci. Adv.* **9**, eade3889 (2023).
19. J. A. Goldbogen *et al.*, Extreme bradycardia and tachycardia in the world's largest animal. *Proc. Natl. Acad. Sci. U.S.A.* **116**, 25329–25332 (2019).
20. D. Thompson, M. A. Fedak, Cardiac responses of grey seals during diving at sea. *J. Exp. Biol.* **16**, 139–154 (1993).
21. J. U. Meir, T. K. Stockard, C. L. Williams, K. V. Ponganis, P. J. Ponganis, Heart rate regulation and extreme bradycardia in diving emperor penguins. *J. Exp. Biol.* **211**, 1169–1179 (2008).
22. T. M. Williams, G. L. Kooyman, D. A. Croll, The effect of submergence on heart rate and oxygen consumption of swimming seals and sea lions. *J. Comp. Physiol. B* **160**, 637–644 (1991).
23. S. R. Kahane-Rapport *et al.*, Lunge filter feeding biomechanics constrain rorqual foraging ecology across scale. *J. Exp. Biol.* **223**, jeb224196 (2020).
24. S. Helbo, A. Fago, Functional properties of myoglobins from five whale species with different diving capacities. *J. Exp. Biol.* **215**, 3403–3410 (2012).
25. S. R. Noren, T. M. Williams, Body size and skeletal muscle myoglobin of cetaceans: Adaptations for maximizing dive duration. *Comp. Biochem. Physiol. A Mol. Integr. Physiol.* **126**, 181–191 (2000).
26. D. E. Cade *et al.*, Tools for integrating inertial sensor data with video bio-loggers, including estimation of animal orientation, motion, and position. *Anim. Biotelem.* **9**, 34 (2021).
27. P. J. Ponganis, G. L. Kooyman, Heart rate and electrocardiogram characteristics of a young california gray whale (Eschrichtius Robustus). *Mar. Mamm. Sci.* **15**, 1198–1207 (1999).
28. R. D. Andrews *et al.*, Heart rates of northern elephant seals diving at sea and resting on the beach. *J. Exp. Biol.* **200**, 2083–2095 (1997).
29. M. A. Castellini *et al.*, Patterns of respiration and heart rate during wakefulness and sleep in elephant seal pups. *Am. J. Physiol. Regul. Integr. Comp. Physiol.* **266**, R863–R869 (1994).
30. S. Ridgway, Homeostasis in the aquatic environment. *Mammals of the Sea*, 590–747 (1972).
31. W. R. Stahl, Scaling of respiratory variables in mammals. *J. Appl. Physiol.* **22**, 453–460 (1967).
32. W. Burggren, A. Fahlman, W. Milsom, Breathing patterns and associated cardiovascular changes in intermittently breathing animals: (Partially) correcting a semantic quagmire. *Exp. Physiol.* **109**, 1051–1065 (2024).
33. A. Fahlman *et al.*, Phylogenetic allometric scaling of near basal breathing frequency in terrestrial, semi-aquatic and aquatic mammals. *Exp. Physiol.* **110**, 1349–1357 (2025).
34. L. Bejder *et al.*, Low energy expenditure and resting behaviour of humpback whale mother-calf pairs highlights conservation importance of sheltered breeding areas. *Sci. Rep.* **9**, 771 (2019).
35. R. L. Storlund *et al.*, Heart rates of Steller sea lions drop slowly and oscillate while diving. *J. Comp. Physiol. B* **196**, 91–103 (2026).
36. D. E. Cade, K. R. Barr, J. Calambokidis, A. S. Friedlaender, J. A. Goldbogen, Determining forward speed from accelerometer jiggle in aquatic environments. *J. Exp. Biol.* **221**, jeb170449 (2018).
37. L. Cipryan, G. Tschakert, P. Hofmann, Acute and post-exercise physiological responses to high-intensity interval training in endurance and sprint athletes. *J. Sports Sci. Med.* **16**, 219–229 (2017).
38. G. C. Bogdanis, M. E. Nevill, L. H. Boobis, H. K. Lakomy, Contribution of phosphocreatine and aerobic metabolism to energy supply during repeated sprint exercise. *J. Appl. Physiol.* **1985**, 876–884 (1996).
39. R. C. Harris *et al.*, The time course of phosphorylcreatine resynthesis during recovery of the quadriceps muscle in man. *Pflugers Arch.* **367**, 137–142 (1976).
40. E. Hultman, J. Bergström, N. M. Anderson, Breakdown and resynthesis of phosphorylcreatine and adenosine triphosphate in connection with muscular work in man. *Scand. J. Clin. Lab. Invest.* **19**, 56–66 (1967).
41. E. C. Nazario *et al.*, Effects of carbon dioxide accumulation on post-dive physiological recovery in odontocetes. *J. Exp. Biol.* **229**, jeb251853 (2026).
42. J. A. Goldbogen *et al.*, Prey density and distribution drive the three-dimensional foraging strategies of the largest filter feeder. *Funct. Ecol.* **29**, 951–961 (2015).
43. P. J. Ponganis, G. L. Kooyman, L. M. Winter, L. N. Starke, Heart rate and plasma lactate responses during submerged swimming and trained diving in California sea lions, Zalophus californianus. *J. Comp. Physiol. B Biochem. Syst. Environ. Physiol.* **167**, 9–16 (1997).
44. M. Kleiber, Body size and metabolism. *Hilgardia* **6**, 315–353 (1932).
45. D. P. Costa, T. M. Williams, "Marine mammal energetics" in *Biology of Marine Mammals*, J. E. Reynolds, S. A. Rommel, Eds. (Smithsonian Institution, 1999).
46. D. R. Powers, K. A. Nagy, Field metabolic rate and food consumption by free-living Anna's hummingbirds (*Calypte anna*). *Physiol. Zool.* **61**, 500–506 (1988).
47. C. C. Peterson, K. A. Nagy, J. Diamond, Sustained metabolic scope. *Proc. Natl. Acad. Sci. U.S.A.* **87**, 2324–2328 (1990).
48. M. A. Castellini, G. L. Kooyman, P. J. Ponganis, Metabolic rates of freely diving Weddell seals: Correlations with oxygen stores, swim velocity and diving duration. *J. Exp. Biol.* **165**, 181–194 (1992).
49. J. L. Maresh *et al.*, Free-swimming northern elephant seals have low field metabolic rates that are sensitive to an increased cost of transport. *J. Exp. Biol.* **217**, 1485–1495 (2014).
50. J. Potvin, J. A. Goldbogen, R. E. Shadwick, Metabolic expenditures of lunge feeding rorquals across scale: Implications for the evolution of filter feeding and the limits to maximum body size. *PLoS ONE* **7**, e44854 (2012).
51. A. M. Blawas, D. P. Nowacek, J. Rocho-Levine, T. R. Robeck, A. Fahlman, Scaling of heart rate with breathing frequency and body mass in cetaceans. *Philos. Trans. R. Soc. B Biol. Sci.* **376**, 20200223 (2021).
52. M. A. Castellini, T. Zenteno-Savin, Heart rate scaling with body mass in pinnipeds. *Mar. Mamm. Sci.* **13**, 149–155 (1997).
53. S. C. Walpole *et al.*, The weight of nations: An estimation of adult human biomass. *BMC Public Health* **12**, 439 (2012).
54. C. Lockyer, Body weights of some species of large whales. *ICES J. Mar. Sci.* **36**, 259–273 (1976).
55. D. E. Cade *et al.*, Minke whale feeding rate limitations suggest constraints on the minimum body size for engulfment filtration feeding. *Nat. Ecol. Evol.* **7**, 535–546 (2023).
56. E. R. Weibel, L. D. Bacigalupe, B. Schmitt, H. Hoppeler, Allometric scaling of maximal metabolic rate in mammals: Muscle aerobic capacity as determinant factor. *Respir. Physiol. Neurobiol.* **140**, 115–132 (2004).
57. B. I. McDonald, M. Johnson, P. T. Madsen, Dive heart rate in harbour porpoises is influenced by exercise and expectations. *J. Exp. Biol.* **221**, jeb168740 (2018).

Downloaded from https://www.pnas.org by 174.61.233.38 on July 27, 2026 from IP address 174.61.233.38.

58. B. I. McDonald, P. J. Ponganis, Deep-diving sea lions exhibit extreme bradycardia in long-duration dives. *J. Exp. Biol.* **217**, 1525–1534 (2014).
59. S. R. Noren, T. Kendall, V. Cuccurullo, T. M. Williams, The dive response redefined: Underwater behavior influences cardiac variability in freely diving dolphins. *J. Exp. Biol.* **215**, 2735–2741 (2012).
60. G. L. Kooyman, W. B. Campbell, Heart rates in freely diving Weddell seal (Leptonychotes weddelli). *Comp. Biochem. Physiol. A Physiol.* **43**, 31–36 (1972).
61. M. A. Hindell, M. A. Lea, Heart rate, swimming speed, and estimated oxygen consumption of a free-ranging southern elephant seal. *Physiol. Zool.* **71**, 74–84 (1998).
62. J. A. Goldbogen *et al.*, Mechanics, hydrodynamics and energetics of blue whale lunge feeding: Efficiency dependence on krill density. *J. Exp. Biol.* **214**, 131–146 (2011).
63. F. Christiansen *et al.*, Maternal body size and condition determine calf growth rates in southern right whales. *Mar. Ecol. Prog. Ser.* **592**, 267–281 (2018).
64. P. S. Segre, A practical guide for improving confidence in data collected with consumer-level drones. *Mar. Mamm. Sci.* **41**, e70022 (2025).
65. W. I. Torres, K. Bierlich, MorphoMetriX: A photogrammetric measurement GUI for morphometric analysis of megafauna. *J. Open Source Softw.* **5**, 1825 (2020).
66. M. van Aswegen *et al.*, Age-specific body length, mass, and energetic cost of growth in humpback whales. *Mar. Ecol. Prog. Ser.* **770**, 171–194 (2025).
67. A. M. Blawas, Respdetect: A Matlab tool for detecting breath events from whale biologger data. *J. Open Source Softw.* **10**, 7858 (2025).
68. J. A. Goldbogen *et al.*, Foraging behavior of humpback whales: Kinematic and respiratory patterns suggest a high cost for a lunge. *J. Exp. Biol.* **211**, 3712–3719 (2008).
69. R Core Team, *R: A Language and Environment for Statistical Computing* (R Core Team, 2020).
70. S. Wood, *mgcv: GAMs and Generalized Ridge Regression for R* (R News 1.2, 2001).
71. A. Blawas, Data for "Sprint-like cardiac dynamics support repeated acrobatic lunges in foraging rorqual whales." Stanford Digital Repository. https://doi.org/10.25740/gc221hc9325. Deposited 29 June 2026.

Downloaded from https://www.pnas.org by 174.61.233.38 on July 27, 2026 from IP address 174.61.233.38.